




Utilization of camalote grass (*Paspalum fasciculatum* Willd. Ex Flüggé) for biosilica recovery through green pretreatment and thermal processing

Aprovechamiento del pasto camalote (*Paspalum fasciculatum* Willd. Ex Flüggé) para la recuperación de biosilíce mediante pretratamiento verde y preprocesamiento térmico

José Pablo Cortazar-Romero¹ , Cintya Valerio-Cárdenas^{1*} , Zaritma Yamilet Montejo-García² 

¹ Universidad Popular de la Chontalpa, División de Ciencias Básicas e Ingenierías, km 2 carretera Cárdenas-Huimanguillo, Ranchería Paso y Playa, 86597, Cárdenas, Tabasco, México.

² Universidad Juárez Autónoma de Tabasco, División Académica Multidisciplinaria de Jalpa de Méndez, Avenida Universidad s/n, Zona de la Cultura, Col. Magisterial, 86040, Villahermosa, Centro, Tabasco, México.

*Corresponding author: cintya.valerio@upch.mx

Reception date:

September 10th, 2025

Acceptation date:

March 5th, 2026

Published on line:

May 5th, 2026

This is an open-access article distributed under the terms of the Creative Commons Attribution License.



Attribution-

NonCommercial-

ShareAlike 4.0

International

(CC BY-NC-SA 4.0)

How to cite:

Cortazar-Romero, J. P., Valerio-Cárdenas, C., & Montejo-García, Z. Y. (2025). Utilization of camalote grass (*Paspalum fasciculatum* Willd. Ex Flüggé) for biosilica recovery through green pretreatment and thermal processing. *Acta Agrícola y Pecuaria*, 11(núm. esp. 2), e0111040. https://doi.org/10.30973/aap/2025.11.e0111040

ABSTRACT

Camalote grass (*Paspalum fasciculatum* Willd. Ex Flüggé, Poaceae) is abundant in southeastern Mexico, and its residues are not currently utilized for economic purposes. However, the generated biomass is rich in silica, allowing it to be integrated into value-added processes. Silica has a wide range of applications. In this study, silica was extracted from the root, stem, and leaf of Camalote grass using a thermochemical method. Proximate analyses revealed ash contents of 32.42 % in roots, 7.12 % in stems, and 19.56 % in leaves. The silica present in the ashes was characterized by powder x-ray diffraction (XRD), where a broad band at $2\theta = 22^\circ$ was observed in leaf and stem samples, corresponding to amorphous silica, while sharp peaks at $2\theta = 26.6^\circ$ were detected root-derived silica, indicating crystalline phases. Leaf-derived ash exhibited a higher density of acidic active sites, which is associated with the presence of surface silanol groups (Si-OH).

KEYWORDS

Silica, biomass, x-ray diffraction, acidic active sites.

RESUMEN

El pasto camalote (*Paspalum fasciculatum* Willd. ex Flüggé, Poaceae) es abundante en el sureste de México, y sus residuos actualmente no se utilizan con fines económicos. Sin embargo, la biomasa generada es rica en sílice, lo que permite su integración en procesos de valor agregado. La sílice tiene una amplia gama de aplicaciones. En este estudio, sílice fue extraída de la raíz, el tallo y la hoja del pasto camalote mediante un método termoquímico. Los análisis proximales revelaron contenidos de cenizas de 32.42 % en raíces, 7.12 % en tallos y 19.56 % en hojas. La sílice presente en las cenizas fue caracterizada mediante difracción de rayos x en polvo (XRD), donde se observó una banda amplia a $2\theta = 22^\circ$ en las muestras de hoja y tallo, correspondiente a sílice amorfa, mientras que se detectaron picos definidos a $2\theta = 26.6^\circ$ en la sílice derivada de raíz, lo que indica fases cristalinas. La ceniza derivada de hojas presentó una mayor densidad de sitios activos ácidos, lo cual se asocia con la presencia de grupos silanol superficiales (Si-OH).

PALABRAS CLAVE

Sílice, biomasa, difracción de rayos x, sitios activos ácidos.

INTRODUCTION

Silicon is predominantly found in nature as oxides and silicates (Richmond & Sussmany, 2003). In soils supporting terrestrial plant growth, silicon (Si) concentrations range from 0.1 % to 10 % of dry weight (Ahad et al., 2022). The extent of silicon accumulation in plants has been shown to correlate with the bioavailable silicon species in the soil, as well as with plant age and tissue type (Deshmukh et al., 2020). Plants absorb silicon through their roots as monosilicic acid (H_4SiO_4), the dominant soluble species in soils at pH below 9, typically found at concentrations under 2mM (Mandlik et al., 2020). Once taken up, it undergoes irreversible precipitation throughout the plant as amorphous silica $SiO_2 \cdot nH_2O$ commonly referred to as “opal”, silica gel, or phytoliths in higher plants (Richmond & Sussmany, 2003).

Plants employ specific transporters for silicon uptake and translocation. In rice, for instance, the Lsi1 and Lsi2 transporters play a critical role in facilitating silicon movement from the roots to the shoots (Souri et al., 2021).

There is a growing interest in studying biosilica not only for its functional role in plants (Dhiman et al., 2021), but also for its potential extraction and application in fields such as supercapacitors, biosensors, biomedicine, drug delivery, gene therapy, and as a filler material for elastomers (Nadda & Gupta, 2024). Elanthikkal et al. (2022) successfully extracted silica from date palm ash for use in photocatalytic applications. Similarly, Liang et al. (2020) focused on the production of biosilica nanoparticles derived from fly ash generated by biomass power plants. Sachan et al. (2021) synthesized silica nanoparticles from foliar biomass and assessed their effectiveness in removing heavy metals from synthetic water systems.

Biosilica extraction methods are primarily classified into two categories: thermal combustion and the sol-gel chemical process, both favored for their simplicity and efficiency. These approaches have enabled the recovery of biosilica from various biomass sources, including date palm ash (Elanthikkal et al., 2022), foliar biomass (Sachan et al., 2021), sugarcane bagasse (Morales-Paredes et al., 2023), and rice husk (Carmona et al., 2013).

The combustion method consists of removing organic matter through high-temperature treatment, while silica remains intact due to its thermal stability. In

contrast, the chemical sol-gel process involves reacting biomass-derived silica with NaOH to produce a sodium silicate solution. Upon acidification, typically with an inorganic acid, this solution yields pure silica nanoparticles through precipitation (Singh et al., 2020). Both methods may require acid pretreatment (acid leaching) when high-purity silica is desired. This step aims to efficiently remove metallic impurities at low cost.

Sulfuric acid (H_2SO_4) is the most used reagent (September et al., 2023), although hydrochloric acid (HCl) has also been widely employed. Due to the toxicity and high corrosiveness of these inorganic acids, greener alternatives have been explored during the pretreatment phase, most notably citric acid, valued for its biological origin and organic nature (September et al., 2023). One of the first studies to employ citric acid for biosilica extraction was conducted by Umeda & Kondoh (2008), who treated biomass at 50 °C with 5 % (w/w) citric acid for 15 minutes, achieving 99.14 % purity after combustion at 800 °C. More recently, Maseko et al. (2021), applied citric acid at 80 °C and 7 % (w/w) for 2 hours to agricultural residues, obtaining a purity of 95.4 %.

This study focused on Camalote grass (*Paspalum fasciculatum* Willd. Ex Flügge, Poaceae) known for producing substantial quantities of silicophytoliths, which can account for approximately 1 % to 10 % of its dry weight. These biogenic silica deposits contribute to structural reinforcement, tolerance to abiotic and biotic stresses, and protection against herbivores, while also representing a renewable source of silica with potential applications in agriculture and materials science (Paolicchi et al., 2019). Silicon is known to accumulate in the roots of Poaceae species, with the endodermis identified as the most common site of silicification (Mandlik et al., 2020).

Paspalum fasciculatum is a perennial grass classified as a difficult-to-control weed (Chacón & Gliessman, 1982). Although its use in bovine feed has been considered, its consumption remains limited. In the absence of proper management, it grows spontaneously, invading and displacing cultivated pastures. As a result, in certain regions it is regarded as a weed (Enríquez Quiroz et al., 2015), and its disposal is often limited to incineration or accumulation in large quantities without any productive use (Valerio-Cárdenas et al., 2024).

This study focuses on the extraction and characterization of biosilica present in the root, leaves, and stems of the Camalote grass, using thermal combustion combined with citric acid as a leaching agent.

MATERIALS AND METHODS

Camalote grass was collected at the end of the winter season in the vicinity of the Universidad Popular de la Chontalpa, located in the municipality of Cárdenas, Tabasco, México (17°53'36" N, 93°21'59" W). According to the Koppen-García climate classification, the study area corresponds to a warm humid climate (Am), characterized by high annual temperatures and abundant rainfall. Plants samples were selected based on maturity to ensure consistency in the analysis. Three independent biological replicates were collected, and each sample was separated into root, stem, and leaf components for individual evaluation.

Drying of plant material

The collected Camalote grass was subjected to solar drying for seven days under average ambient temperatures of 32 °C until constant weight was achieved. Samples were weighed every two days to monitor moisture loss. The general procedure is illustrated in Figure 1.

Subsequently, the plant material was separated into morphological sections (root, stem, and leaf) to estimate residual moisture distribution across each segment. Each section was placed in an Eco-Shell muffle furnace (model eco-7L Rorer, Ciudad de México, México), raking volume of 7 L. Thermal treatment was conducted at 120 ± 2 °C for two hours under conditions of uniform heat distribution and temperature stability within ± 1 °C. The same equipment was used for subsequent thermal analyses.

Proximate analysis

Proximate analysis (moisture, volatile matter, ash content, and fixed carbon) were determined by the standard method D3172-13 (Reapproved 2021)^{e1} (ASTM, 2021). Moisture content was determined by oven-drying at 105 °C until constant weight. Volatile matter was obtained by muffle furnace at 400 °C for four hours, while ash content was obtained by muffle furnace combustion at 800 °C for four hours. Fixed carbon (FC) was calculated using the formula:

$$FC = 100 - (\text{Moisture} + \text{Ash} + \text{Volatile Matter})$$

All measurements were performed on the dried root, stem, and leaf fractions of Camalote grass, ensuring consistency across anatomical segments.

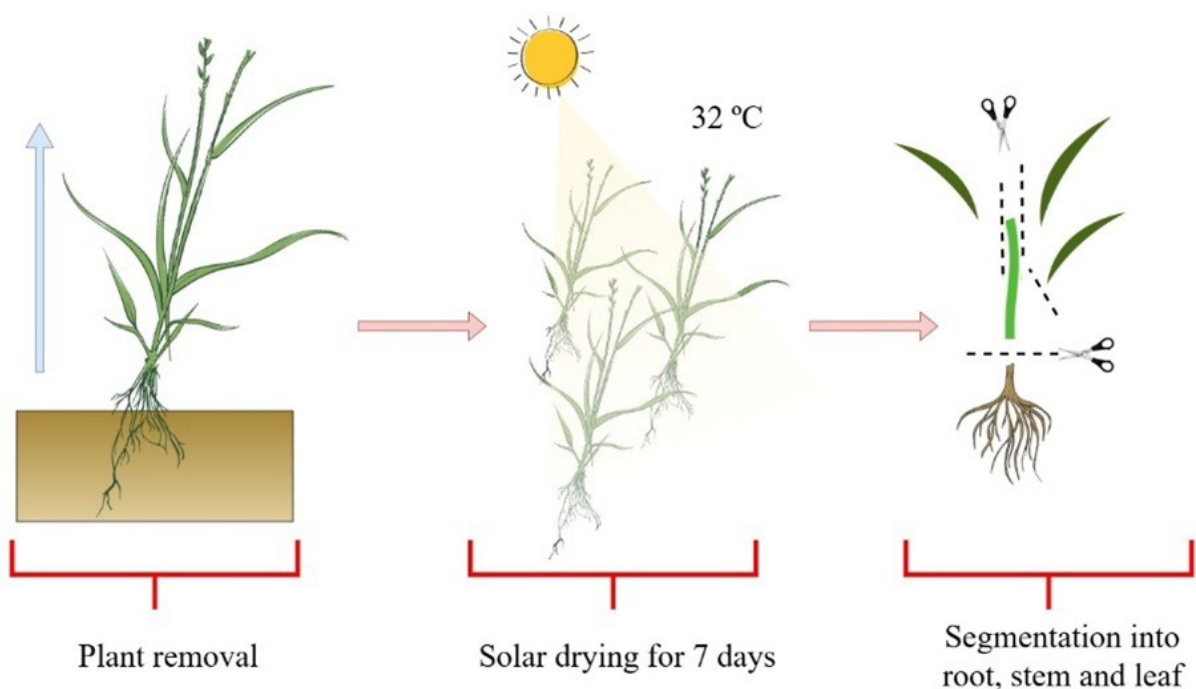


Figure 1. General procedure for plant collection, solar drying, and anatomical segmentation.

Biosilica extraction

The plant material was subjected to two experimental methods to evaluate the efficiency of temperature and leaching agents during the pretreatment phase for biosilica extraction, as detailed below.

Method A: five grams of dry plant material were treated with boiling ethanol for 1 h to remove organic residues. The sample was then carbonized at 400 °C for 2 h. The resulting ash was treated with 5 % citric acid to leach mineral impurities, followed by two rinsing cycles with distilled water to remove residual acid and soluble compounds. A final combustion step was performed at 800 °C. Initial and final weights were recorded after each combustion stage to assess mass reduction and silica yield.

Method B: five grams of dry plant material were treated with 5 % citric acid at 60 °C for 30 minutes. The sample then underwent two rinsing cycles with distilled water, followed by drying. Subsequently, the material was combusted at 800 °C for 5 h. Initial and final weights were recorded to evaluate mass reduction and biosilica yield.

The recorded weights were used to calculate the biosilica content (%) in the leaf, root, and stem of Camalote grass, according to Equation 1:

$$\%Biosilica = \frac{F_w}{I_w} 100 \quad \text{Eq. 1}$$

Where:

I_w : Initial dry weight of the material.

F_w : Final weight of the material after combustion.

Active sites

An adapted version of the Boehm (1966) method was employed to quantify the surface acidic and basic sites present in the biosilica. For each assay, 0.1 g of sample was mixed with 25 mL of 0.1 N titrant solution: hydrochloric acid (HCl) for the determination basic sites, and sodium hydroxide (NaOH) for acidic sites. The mixtures were maintained at 25 °C for five days, with agitation at 300 rpm applied twice daily. After the interaction period, supernatants were filtered and titrated with the corresponding counter-solution

(NaOH for HCl-treated samples and HCl for NaOH-treated samples) using phenolphthalein as an indicator. The concentration of surface functional groups was calculated in milliequivalents per gram (meq/g) using Equation 2:

$$C_{sa} = \frac{V_{in} (C_{in} - C_{fn})}{m} \times 1000 \quad \text{Eq. 2}$$

Where:

C_{sa} = concentration of active sites meq/g.

C_{in} = initial concentration of the neutralizing solution (eq/L).

C_{fn} = final concentration of the neutralizing solution (eq/L).

m = mass of the biosilica sample (g).

V_{in} = volumen of neutralizing solution (L).

The final concentration of the neutralizing solution was estimated using Equation 3:

$$C_{fn} = \frac{V_T C_T}{V_m} \quad \text{Eq. 3}$$

Where:

C_T = concentration of the titrant solution (eq/L)

V_T = volume of titrant used (L)

V_m = volume of neutralizing solution (L)

Elemental analysis

The chemical composition of both raw Camalote grass and its ash fractions was determined using energy-dispersive x-ray spectroscopy (EDX) coupled with a variable-pressure scanning electron microscope (VP-SEM, JSM-6360 LV, JEOL, Tokyo, Japan). This technique enabled qualitative and semi-quantitative identification of elemental constituents, providing insight into the distribution and concentration of silicon and other relevant elements in the biosilica matrix.

x-ray diffraction analysis

The structural patterns of the biosilica samples were examined using BRUKER D8-ADVANCE diffractometer (Massachusetts, USA) configured in Bragg-Brentano reflection geometry (θ - 2θ). Measurements were performed using Cu-K α_1 radiation ($\lambda = 1.5406 \text{ \AA}$), under operating conditions of 34 kV and 25 mA.

RESULTS AND DISCUSSION

Elemental composition of Camalote grass and its derived ash

The elemental composition data for raw Camalote grass and its ash-derived biosilica are presented in Table 1. Native Camalote is primarily composed of oxygen (52.54 %), associated with both organic constituents (cellulose, hemicellulose, and lignin) and inorganic mineral phases. The silicon content in the raw biomass (9.49 %) reflects the plant's ability to uptake silicon as monosilicic acid and subsequently deposit it as amorphous silica within tissues. This relatively high silicon accumulation is consistent with the behavior of Poaceae species, which are known as silicon accumulators (Rufo et al., 2014).

Following thermal treatment, the marked increase in silicon concentration (25.95 %) and the relative persistence of oxygen (48.61 %) in the ash indicates the removal of organic matter and the enrichment of inorganic siliceous phases. This transformation is characteristic of biomass combustion processes, in which carbonaceous components are oxidized, leaving behind silica-rich residues. The strong correlation between elemental composition and x-ray diffraction patterns supports the formation of predominantly amorphous biosilica, as evidenced by the broad diffraction halos typical of non-crystalline materials.

From a mechanistic perspective, the presence of silicon in association with elements such as aluminum suggests the formation of aluminosilicate complexes, which may influence the thermal stability and structural organization of the resulting ash. These interactions can affect both the purity and reactivity of the recovered biosilica, which are critical parameters for its potential applications.

Differences in silicon accumulation capacity are species-dependent and are further modulated by environmental conditions such as soil composition and water availability. Additionally, thermal treatment parameters—particularly temperature and residence time—play a crucial role in determining the degree of organic matter removal and the crystallinity of the resulting silica. For instance, studies such as Morales-Paredes et al. (2023) and Oo et al. (2021) report

significant variation in elemental composition, which can be attributed to these combined effects.

Table 1. Elemental composition (% weight) of raw Camalote and its ash-derived biosilica.

Element	Raw Camalote	Ash-derived
O	52.54 %	48.61 %
Si	9.49 %	25.95 %
K	1.24 %	11.76 %
C	36.24 %	6.14 %
Mg	----	2.99 %
S	0.25 %	2.38 %
Ca	----	1.10 %
Na	----	0.50 %
Al	----	0.40 %
P	----	0.16 %
Cl	0.23 %	----

Proximate composition of leaf, stem, and root fractions

Moisture loss in various biomass types typically occurs within a temperature range of 25 °C to 140 °C (Varol & Mutlu, 2023). In the case of Camalote grass, air drying for five days at an average environment temperature of 38 °C resulted in approximately 50 % water removal. This dehydration process was accompanied by visible discoloration of the plant material (Figure 2), suggesting structural and compositional changes associated with moisture reduction and partial degradation of organic compounds.

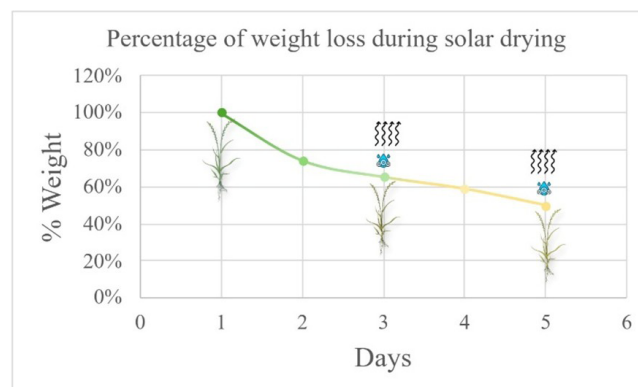


Figure 2. Mass loss of Camalote grass during five days of air-drying at room temperature.

Table 2. Proximate analysis of Camalote grass.

Section	% moisture	% ash	% volatile solids	% fixed carbon
Leaf	7.27 %	19.56 %	18.43 %	54.74 %
Stem	13.71 %	7.12 %	5.95 %	73.22 %
Root	5.84 %	32.42 %	30.66 %	31.08 %

Table 2 presents variations in proximate composition among the anatomical fractions of Camalote grass. The root exhibited the highest ash content (32.42 %), which is consistent with its role in nutrient uptake and accumulation of inorganic elements from the soil. In contrast, the stem showed the lowest ash content (7.12 %), reflecting its primarily structural function and reduced role in mineral storage. The leaf presented intermediate ash values (19.56 %), likely associated with the translocation and temporary storage of minerals. These differences can be partially attributed to the relative composition of lignocellulosic components. In particular, lignin content followed a decreasing trend from root (1.76 %) to stem (1.17 %) and leaf (1.13 %), reflecting functional specialization and tissue composition. This variation in biochemical composition directly influences the thermal behavior and ash yield of each fraction, which is relevant for optimizing biomass processing and biosilica recovery.

Ash content and thermal behavior of Camalote grass fractions

Figure 3 presents the mass loss and ash content results obtained from Camalote grass fractions using two dif-

ferent processing approaches (Methods A and B). In Method A, thermal treatment at 400 °C resulted in substantial mass loss across all anatomical sections. Leaf samples exhibited approximately 80 % mass reduction under both ethanol-treated and untreated conditions, while stem samples showed a more pronounced loss of nearly 93 %. Root samples displayed comparatively lower mass losses of 66 % and 58 % for ethanol-treated and untreated conditions, respectively. This behavior is consistent with the thermal decomposition of cellulose and hemicellulose, which predominantly occurs within this temperature range (Yang et al., 2007), indicating that the observed mass loss is largely associated with the degradation of structural polysaccharides. Following citric acid treatment and calcination at 600 °C, significant differences in mass retention were observed among plant fractions. Leaf samples retained approximately 10 % of their initial mass, whereas stem samples showed minimal residual mass (~1.5 %) regardless of ethanol pretreatment. In contrast, root samples exhibited substantially higher retention values of 28 % and 35 % for ethanol-treated and untreated samples, respectively. Considering that most organic and extractable components are removed during thermal processing, the residual mass is primarily attributed

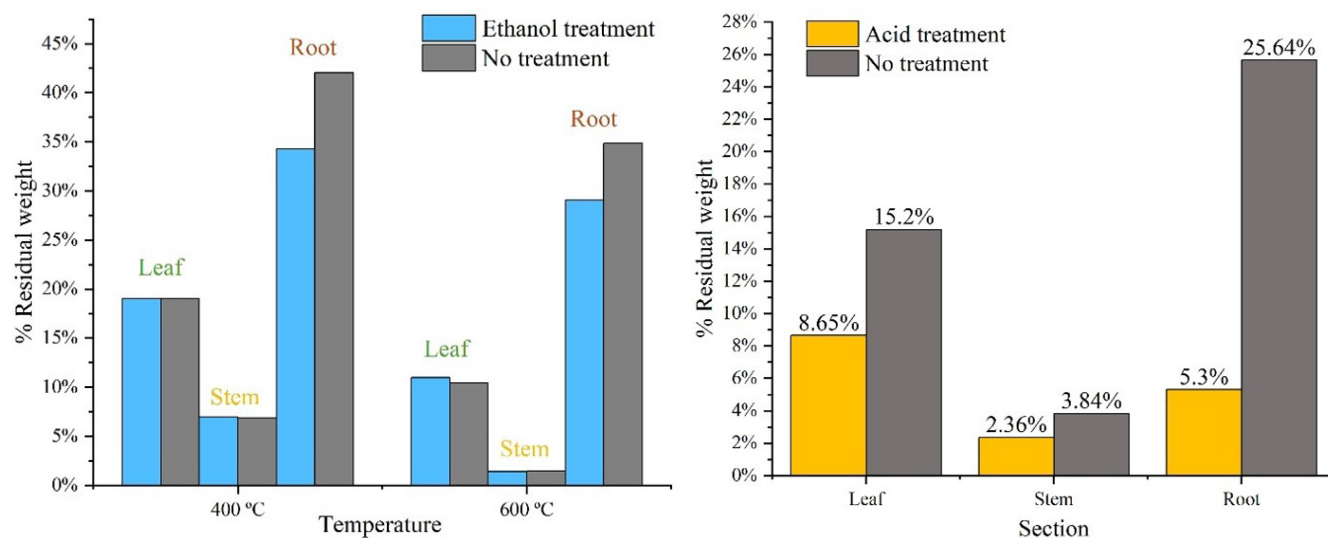


Figure 3. Ash yield obtained across anatomical sections: (a) Method A and (b) Method B.

to inorganic constituents, particularly biosilica. This is supported by the high thermal stability of silica, which remains stable under these conditions. Ethanol pretreatment did not significantly influence mass loss in leaf and stem fractions; however, slight differences observed in root samples suggest the removal of adhered soil particles and impurities, which are more prevalent in belowground biomass.

In Method B, the effect of citric acid treatment on ash content was more pronounced. Untreated samples exhibited ash contents of 15.20 % (leaf), 3.84 % (stem), and 25.64 % (root). After acid treatment, these values decreased to 8.65 %, 2.36 %, and 5.30 %, respectively. The most significant reduction was observed in the root fraction, indicating effective removal of mineral impurities such as soil residues and loosely bound inorganic components during acid leaching. The relatively minor change in the stem fraction suggests a lower content of extractable inorganic materials. These findings highlight the influence of pretreatment strategies on ash yield and composition. While Method A primarily reflects the thermal degradation behavior and intrinsic mineral content of the biomass, Method B demonstrated the effectiveness of acid leaching in reducing inorganic impurities and improving the purity of the resulting biosilica. Comparable trends have been reported by Teixeira et al. (2021), who observed variations in ash content in sugarcane-derived biomass depending on the applied thermochemical treatments.

Ash color and visual characteristics

The color of the ash samples obtained through both methods is summarized in Figure 4. At 600 °C (Method A), leaf-derived ashes exhibited a light beige tone under both treatment conditions, suggesting the presence of residual lignin, whose thermal degradation occurs between 170 °C and 945 °C (Varol & Mutlu, 2023), with partial persistence above 500 °C (El-Sayed et al., 2024). Stem ashes also displayed a light beige hue; however, some replicates showed a grayish tint, likely resulting from incomplete combustion or the presence of residual impurities. Under both treatment conditions, root-derived ashes exhibited a distinct earthy brown coloration, which may be caused by the presence of mineral constituents, particularly iron compounds.

At 800 °C, leaf-derived ashes exhibited a distinct white coloration. Samples subjected to citric acid pretreatment produced brighter white ashes, whereas untreated leaves retained a grayish-white tone. According to Singh & Endley (2020), ash whiteness can be used as a preliminary indicator of metallic impurity removal through acid leaching, a criterion further supported by Elanthikkal et al. (2022).

Stem-derived ashes consistently displayed dark gray tones, regardless of pretreatment, suggesting a limited effect of acid washing on residual coloration in this fraction. In contrast, root-derived ashes showed a slight increase in brightness compared to those obtained at 600 °C, with a more noticeable effect in citric acid-treated samples. This change may be associated with the partial removal of surface-bound minerals, particularly iron compounds during the leaching process.

x-ray diffraction (XRD) analysis

The XRD patterns obtained from leaf, stem, and root ashes revealed structural differences associated with combustion conditions and applied treatments. Biosilica, typically present as amorphous silica, is characterized by a broad, asymmetric diffraction peak within the range of $18^\circ \leq 2\theta \leq 28^\circ$, without sharp crystalline reflections (Schneider et al., 2018). This feature reflects the non-crystalline nature of the material and serves as a key indicator for assessing the structural purity of the samples. Figure 5 shows the XRD pattern of leaf-derived ashes. Under Method B, samples subjected to citric acid pretreatment and calcined at 800 °C exhibited a broad characteristic peak within the range of $15^\circ \leq 2\theta \leq 30^\circ$, with a maximum intensity at $2\theta = 22^\circ$. This pattern is consistent with previous studies on sugarcane bagasse ashes (Chindaprasirt & Rattanasak, 2020; Teixeira et al. 2021), confirming the presence of amorphous silica. In contrast, untreated leaf ashes calcined at the same temperature displayed less homogeneous diffraction pattern, with sharp and well-defined peaks associated with crystalline phases. This behavior may be influenced by calcination temperature, biomass composition, and combustion conditions (Dizaji et al., 2019). Additionally, metallic impurities present in the biomass have been reported to promote silica crystallization during thermal processing (Setiawan & Chiang, 2021), highlighting the importance of citric acid leaching for impurity removal.

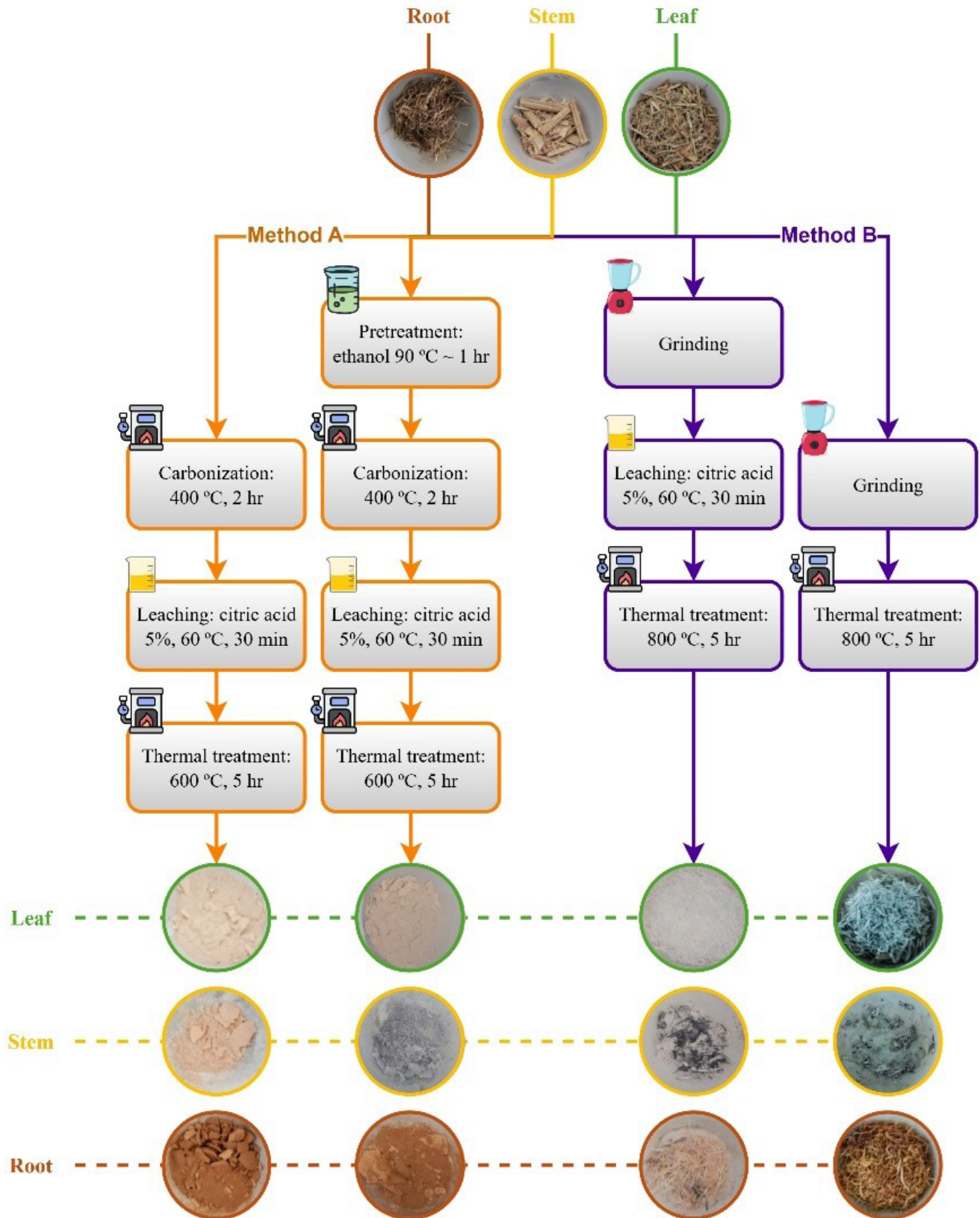


Figure 4. Ash color of Camalote grass obtained by different methods.

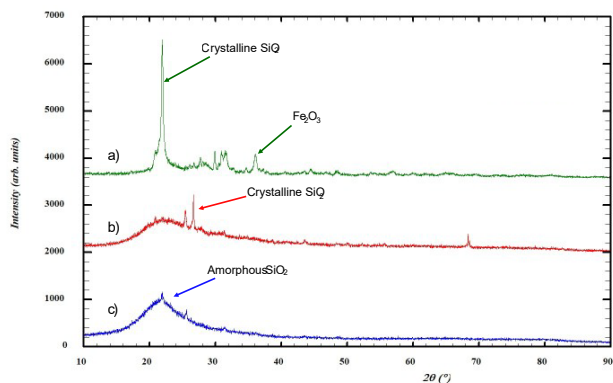


Figure 5. XRD patterns of Camalote grass leaf ash: a) untreated, b) EtOH treated, c) citric acid treated.

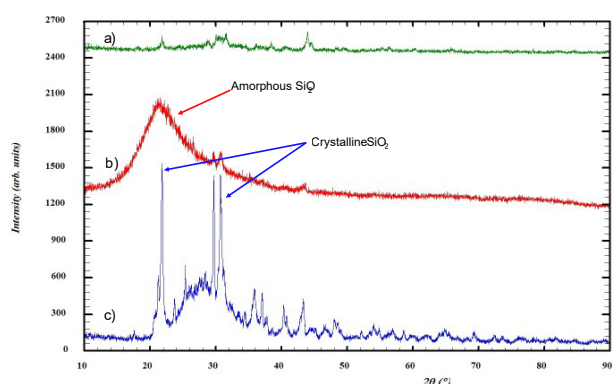


Figure 6. XRD patterns of Camalote grass stem ash: a) untreated, b) EtOH treated, c) citric acid treated.

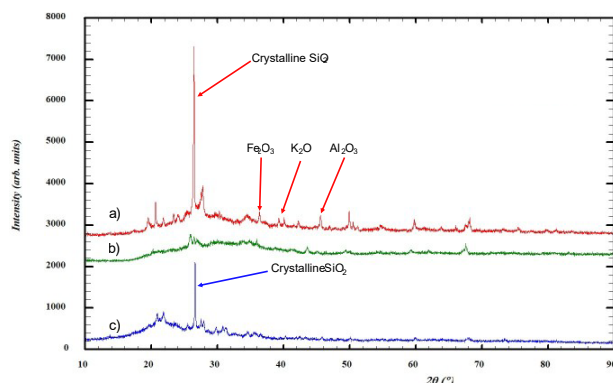


Figure 7. XRD patterns of Camalote grass root ash: a) EtOH treated, b) untreated, c) citric acid treated.

Figure 6 illustrates the XRD profiles of stem-derived ashes under different thermal and chemical conditions. At 800 °C without acid pretreatment, diffraction signals were of low intensity, indicating limited crystallinity. In contrast, samples treated with citric acid and calcined at the same temperature exhibited more defined peaks, suggesting partial crystallization. At 600 °C, following ethanol pretreatment, stem ashes displayed a broad diffraction peak characteristic of amorphous silica.

The XRD profiles of root-derived ashes at both 600 °C and 800 °C showed intense and well-defined peaks, indicative of a predominantly crystalline structure. As shown in Figure 7 additional diffraction signals suggest the presence of inorganic compounds, which is consistent with the observed coloration of the ashes.

Previous studies indicate that temperatures above 800 °C, particularly in the presence of alkali metals such as potassium, promote the formation of crystalline silica phases (Soltani et al., 2014). In contrast, Umeda & Kondoh (2008) reported that amorphous silica can be preserved at temperatures below 1,000 °C under controlled impurity conditions. These findings suggest that biosilica produced via Method B at 800 °C remains predominantly amorphous when acid pretreatment is applied, due to the effective removal of metallic impurities.

Active sites in leaf ashes

Figure 8 shows a predominance of acidic sites (8.25 meq g⁻¹), suggesting that amorphous biosilica is the major component in leaf-derived ash. During combustion, the biogenic silica present in the leaf is transformed into a porous SiO₂ structure, whose surface is enriched with highly polar silanol (Si-OH) groups. These functional groups act as proton donors, accounting for the pronounced acidity of the ash. Basic sites were also detected (4.04 meq g⁻¹), although in lower proportion, indicating that the ash is not composed of pure biosilica. This basicity is likely associated with the presence of metal oxides formed during combustion, which contribute to the overall surface reactivity of the material. Compared to previous studies, the acidity observed in this work is significantly higher. Aneu et al. (2020) reported a maximum acidity of 0.5517 meq g⁻¹ in silica synthesized from tetraethyl orthosilicate, while Moreno & Giraldo (2005) reported an upper value of 0.72 meq g⁻¹ for acidic sites in biochar. These differences highlight the strong influence of thermochemical treatment conditions and biomass origin on the development of surface functional groups. The high density of acidic sites observed in leaf-derived ash suggests a material with significant potential for applications in adsorption, catalysis, and surface modification processes, where surface reactivity plays a critical role.

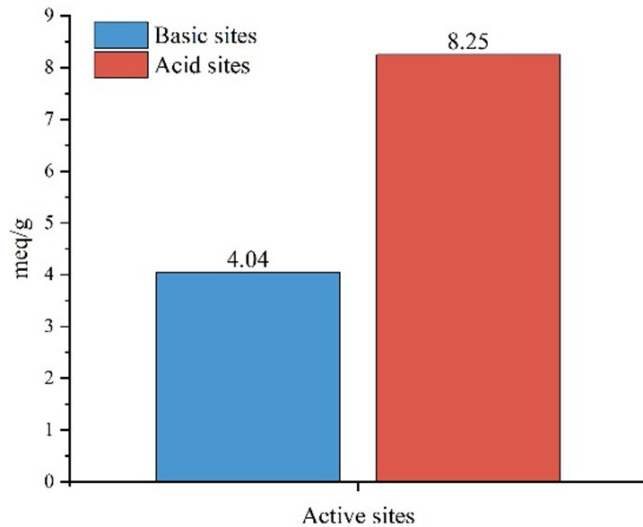


Figure 8. Active sites present in Camalote grass leaf ash obtained by Method B.

CONCLUSIONS

This study demonstrated that Camalote grass is a viable and sustainable source of biosilica, with its anatomical fractions exhibiting distinct physicochemical properties that influence silica recovery.

Thermochemical treatment significantly affected the composition and structure of the resulting ash. The increase in silicon concentration after calcination, together with xRD analysis, confirmed the formation of predominantly amorphous biosilica, particularly in leaf-derived samples. Acid pretreatment proved to be a key factor in enhancing biosilica purity by removing metallic impurities that otherwise promote crystallization.

Among the evaluated fractions, leaves showed the most favorable characteristics for biosilica production, including a higher proportion of amorphous silica structures, lighter ash coloration, and a high density of acidic surface sites. In contrast, root-derived ash exhibited higher impurity content and a greater presence of crystalline phases, likely associated with mineral accumulation from the soil.

The abundance of silanol groups in leaf ash resulted in a high density of acidic sites, indicating strong potential for applications in adsorption, catalysis, and surface modification processes. Overall, the results highlight the importance of biomass fractions selection and pretreatment strategies in optimizing biosilica recovery from lignocellulosic materials.

Method B, based on citric acid pretreatment, proved to be the most effective approach for impurity removal and biosilica purification, particularly at 800 °C. These findings support the use of Camalote grass as a low-cost and renewable material for the production of value-added silica-based materials.

ACKNOWLEDGMENTS

To the Secretaría de Ciencias y Humanidades, Tecnología e Innovación (Mexico) for the scholarship granted under cvu No. 2065078. We are grateful to the Laboratorio Nacional de Nano y Biomateriales (CINVESTAV-Merida) for EDX analyses.

LITERATURE CITED

- Ahad, A., Ahmad, N., Ilyas, M., Batool, T. S., & Gul, A. (2022). Plant metal and metalloid transporters. En K. Kumar & S. Srivastava (Eds.), *Plant Metal and Metalloid Transporters* (pp. 1-21). Springer.
- Aneu, A., Wijaya, K., & Syoufian, A. (2020). Silica-based solid acid catalyst with different concentration of H₂SO₄ and calcination temperature: Preparation and characterization. *Silicon*, 13, 2265-2270. <https://doi.org/10.1007/s12633-020-00741-6>
- ASTM International (2021). *D3172-13 (Reapproved 2021) e1. Standard Practice for Proximate Analysis of Coal and Coke*. ASTM International. <https://doi.org/10.1520/D3172-13R21E01>
- Boehm, H. P. (1966). Chemical identification of surface groups. *Advances in Catalysis*, 16, 179-274. [https://doi.org/10.1016/S0360-0564\(08\)60354-5](https://doi.org/10.1016/S0360-0564(08)60354-5)
- Carmona, V. B., Oliveira, R. M., Silva, W. T. L., Mattoso, L. H. C., & Marconcini, J. M. (2013). Nanosilica from rice husk: Extraction and characterization. *Industrial Crops and Products*, 43, 291-296. <https://doi.org/10.1016/j.indcrop.2012.06.050>
- Chacón, J. C., & Gliessman, S. R. (1982). Use of the “non-weed” concept in traditional tropical agroecosystems of south-eastern Mexico. *Agro-Ecosystems*, 8(1), 1-11. [https://doi.org/10.1016/0304-3746\(82\)90010-5](https://doi.org/10.1016/0304-3746(82)90010-5)
- Chindaprasirt, P., & Rattanasak, U. (2020). Eco-production of silica from sugarcane bagasse ash for use as a photochromic pigment filler. *Scientific Reports*, 10, 9890. <https://doi.org/10.1038/s41598-020-66885-y>

- Deshmukh, R., Sonah, H., & Belanger, R. R. (2020). New evidence defining the evolutionary path of aquaporins regulating silicon uptake in land plants. *Journal of Experimental Botany*, 71(21), 6775-6788. <https://doi.org/10.1093/jxb/eraa342>
- Dhiman, P., Rajora, N., Bhardwaj, S., Sudhakaran, S. S., Kumar, A., Raturi, G., Chakraborty, K., Gupta, O. P., Devanna, B. N., Tripathi, D. K., & Deshmukh, R. (2021). Fascinating role of silicon to combat salinity stress in plants: An updated overview. *Plant Physiology and Biochemistry*, 162, 110-123. <https://doi.org/10.1016/j.plaphy.2021.02.023>
- Dizaji, H. B., Zeng, T., Hartmann, I., Enke, D., Schliermann, T., Lenz, V., & Bidabadi, M. (2019). Generation of high quality biogenic silica by combustion of rice husk and rice straw combined with pre- and post-treatment strategies—A review. *Applied sciences*, 9(6), 1083. <https://doi.org/10.3390/app9061083>
- Elanthikkal, S., Mohamed, H. H., & Alomair, N. A. (2022). Extraction of biosilica from date palm biomass ash and its application in photocatalysis in photocatalysis. *Arabian Journal of Chemistry*, 16, 104522. <https://doi.org/10.1016/j.arabjc.2022.104522>
- El-Sayed, S. A., Khass, T. M., & Mostafa, M. E. (2024). Thermal degradation behaviour and chemical kinetic characteristics of biomass pyrolysis using TG/DTC/DTA techniques. *Biomass Conversion and Biorefinery*, 14, 17779-17803. <https://doi.org/10.1007/s13399-023-03926-2>
- Enríquez Quiroz, J. F., Hernández Garay, A., Queo Carrillo, A. R., & Martínez Méndez, D. (2015). *Producción y manejo de gramíneas tropicales para pastoreo en zonas*. Instituto Nacional de Investigación Forestal, Agrícola y Pecuaria; Colegio de Postgraduados.
- Liang, G., Li, Y., Yang, C., Zi, C., Zhang, Y., Hu, X., & Zhao, W. (2020). Production of biosilica nanoparticles from biomass power plant fly ash. *Waste Management*, 105, 8-17. <https://doi.org/10.1016/j.wasman.2020.01.033>
- Mandlik, R., Thakral, V., Raturi, G., Shinde, S., Nikolić, M., Tripathi, D. K., Sonah, H., & Deshmukh, R. (2020). Significance of silicon uptake, transport, and deposition in plants. *Journal of Experimental Botany*, 71(21), 6703-6718. <https://doi.org/10.1093/jxb/eraa301>
- Maseko, N. N., Schneider, D., Wassersleben, S., Enke, D., Iwarere, S. A., Pocock, J., & Stark, A. (2021). The production of biogenic silica from different South African agricultural residues through a thermo-chemical treatment method. *Sustainability*, 13(2), 577.
- Morales-Paredes, C. A., Rodríguez-Linzán, I., Saquete, M. D., Luque, R., Osman, S. M., Boluda-Botella, N., & Rodríguez-Díaz, J. M. (2023). Silica-derived materials from agro-industrial waste biomass: Characterization and comparative studies. *Environmental Research*, 231(Part 1), 116002. <https://doi.org/10.1016/j.envres.2023.116002>
- Moreno, J. C., & Giraldo, L. (2005). Correlación entre la acidez y la basicidad total de carbones activados y la entalpía de inmersión en disoluciones de ácidos y bases. *Revista CENIC Ciencias Químicas*, 37(3), 169-171.
- Nadda, A. K., & Gupta, V. K. (Edits.). (2024). *Biogenic Silica: Fundamentals and Applications*. Royal Society of Chemistry. <https://doi.org/10.1039/9781839169717>
- Oo, H. M., Karin, P., Chollacoop, N., & Hanamura, K. (2021). Physicochemical characterization of forest and sugarcane leaf combustion's particulate matters using electron microscopy, EDS, XRD and TGA. *Journal of Environmental Sciences*, 99, 296-310. <https://doi.org/10.1016/j.jes.2020.06.036>
- Paolicchi, M., Benvenuto, M. L., Honaine, M. F., & Osterrieth, M. (2019). Root silicification of grasses and crops from the Pampean region and its relevance to silica and silicophytolith content of soils. *Plant and Soil*, 444, 351-363. <https://doi.org/10.1007/s11104-019-04287-4>
- Richmond, K. E., & Sussman, M. (2003). Got silicon? The non-essential beneficial plant nutrient. *Current Opinion in Plant Biology*, 26(3), 268-272. [https://doi.org/10.1016/S1369-5266\(03\)00041-4](https://doi.org/10.1016/S1369-5266(03)00041-4)
- Rufo, L., Franco, A., & de la Fuente, V. (2014). Silicon in *Imperata cylindrica* (L.) P. Beauv: content, distribution, and ultrastructure. *Protoplasma*, 251, 921-930. <https://doi.org/10.1007/s00709-013-0594-8>
- Sachan, D., Ramesh, A., & Das, G. (2021). Green synthesis of silica nanoparticles from leaf biomass and its application to remove heavy metals from synthetic wastewater: A comparative analysis. *Environmental Nanotechnology, Monitoring & Management*, 16, 100467. <https://doi.org/10.1016/j.enmm.2021.100467>
- Schneider, D., Wassersleben, S., Weiß, M., Denecke, R., Stark, A., & Enke, D. (2018). A generalized procedure for the production of high-grade, porous biogenic silica. *Waste and Biomass Valorization*, 11, 1-15. <https://doi.org/10.1007/s12649-018-0415-6>
- September, L. A., Kheswa, N., Seroka, N. S., & Khotseng, L. (2023). Green synthesis of silica and silicon from agricultural residue sugarcane bagasse ash – a mini review.

- RSC Advances*, 13, 1370-1380. <https://doi.org/10.1039/D2RA07490G>
- Setiawan, W. K., & Chiang, K.-Y. (2021). Crop residues as potential sustainable precursors for developing silica materials: A review. *Waste and Biomass Valorization*, 12(5), 2207-2236. <https://doi.org/10.1007/s12649-020-01126-x>
- Singh, J., Boddula, R., & Jirimali, H. D. (2020). Utilization of secondary agricultural products for the preparation of value added silica materials and their important applications: a review. *Journal of Sol-Gel Science and Technology*, 96, 15-33. <https://doi.org/10.1007/s10971-020-05353-5>
- Singh, S. P., & Endley, N. (2020). Fabrication of nano-silica from agricultural residue and their application. In A. Husen & M. Jawaid, *Nanomaterials for Agriculture and Forestry Applications* (pp. 107-134). Elsevier. <https://doi.org/10.1016/B978-0-12-817852-2.00005-6>
- Soltani, N., Bahrami, A., Pech-Canul, M. I., & González, L. A. (2014). Review on the physicochemical treatments of rice husk for production of advanced materials. *Chemical Engineering Journal*, 264, 899-935. <https://doi.org/10.1016/j.cej.2014.11.056>
- Souri, Z., Khanna, K., Karimi, N., & Ahmad, P. (2021). Silicon and plants: Current knowledge and future prospects. *Journal of Plant Growth Regulation*, 40, 906-925. <https://doi.org/10.1007/s00344-020-10172-7>
- Teixeira, L. B., de Moraes, E. G., Shinhe, G. P., Falk, G., & de Oliveira, A. P. N. (2021). Obtaining biogenic silica from sugarcane bagasse and leaf ash. *Waste and Biomass Valorization*, 12, 3205-3221. <https://doi.org/10.1007/s12649-020-01230-y>
- Umeda, J., & Kondoh, K. (2008). High-purity amorphous silica originated in rice husks via carboxylic acid leaching process. *Journal of Materials Science*, 43, 7084-7090. <https://doi.org/10.1007/s10853-008-3060-9>
- Valerio-Cárdenas, C., De la Cruz-Burelo, P., Bolio-López, G. I., & Velázquez-Carmona, M. Á. (2024). Efficiency of camalote grass residue (*Paspalum fasciculatum* Willd) in the adsorption of methylene blue. *Revista U.D.C.A Actualidad & Divulgación Científica*, 27(1), e2496. <http://doi.org/10.31910/rudca.v27.n1.2024.2496>
- Varol, E. A., & Mutlu, Ü. (2023). TGA-FTIR analysis of biomass samples based on the thermal decomposition behavior of hemicellulose, cellulose, and lignin. *Energies*, 16(9), 3674. <https://doi.org/10.3390/en16093674>
- Yang, H., Yan, R., Chen, H., Lee, D. H., & Zheng, C. (2007). Characteristics of hemicellulose, cellulose and lignin pyrolysis. *Fuel*, 86(12-13), 1781-1788. <https://doi.org/10.1016/j.fuel.2006.12.013>